

Double parton scattering at high energies *

ANTONI SZCZUREK

Institute of Nuclear Physics PAN, PL-31-342 Cracow, Poland and
University of Rzeszów, PL-35-959 Rzeszów, Poland

We discuss a few examples of rich newly developing field of double parton scattering. We start our presentation from production of two pairs of charm quark-antiquark and argue that it is the golden reaction to study the double parton scattering effects. In addition to the DPS we consider briefly also mechanism of single parton scattering and show that it gives much smaller contribution to the $c\bar{c}c\bar{c}$ final state. Next we discuss a perturbative parton-splitting mechanism which should be included in addition to the conventional DPS mechanism. We show that the presence of this mechanism unavoidably leads to collision energy and other kinematical variables dependence of so-called σ_{eff} parameter being extracted from different experiments. Next we briefly discuss production of four jets. We concentrate on estimation of the contribution of DPS for jets remote in rapidity. Understanding of this contribution is very important in the context of searches for BFKL effects known under the the name Mueller-Navelet jets. We discuss the situation in a more general context. Finally we briefly mention about DPS effects in production of W^+W^- . Outlook closes the presentation.

PACS numbers: 11.80.La,13.87.Ce,14.65.Dw,14.70.Fm

1. Introduction

It is well known that the multi-parton interaction in general and double parton scattering processes in particular become more and more important at high energies. In the present short review we concentrate on double parton processes (DPS) which can be described as perturbative processes, i.e. processes where the hard scale is well defined (production of heavy objects, or objects with large transverse momenta). In general, the cross section for the double-parton scattering grows faster than the corresponding (the same final state) cross section for single parton scattering (SPS).

* Presented at the XXI Cracow EPIPHANY Conference on Future High Energy Colliders

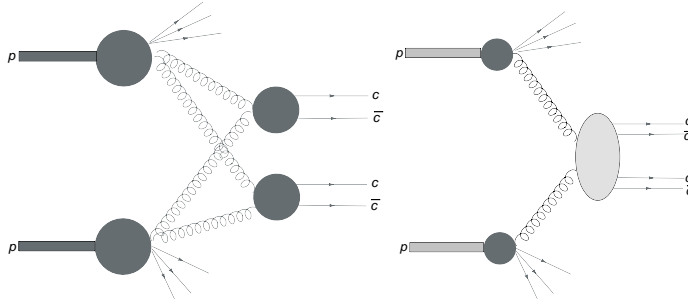


Fig. 1. SPS and DPS production mechanisms of $c\bar{c}c\bar{c}$.

The double-parton scattering was recognized already in seventies and eighties [1, 2, 3, 4, 5, 6, 7, 8, 9]. The activity stopped when it was realized that their contribution at the center-of-mass energies available at those times was negligible. Several estimates of the cross section for different processes have been presented in recent years [10, 11, 12, 13, 14, 15, 16, 17, 18]. The theory of the double-parton scattering is quickly developing (see e.g. [19, 20, 21, 22, 23, 24, 25, 26]).

In Ref. [27] we showed that the production of $c\bar{c}c\bar{c}$ is a very good place to study DPS effects. Here, the quark mass is small enough to assure that the cross section for DPS is very large, and large enough that each of the scatterings can be treated within pQCD.

The calculation performed in Ref. [27] were done in the leading-order (LO) collinear approximation. This may not be sufficient when comparing the results of the calculation with real experimental data. In the meantime the LHCb collaboration presented new interesting data for simultaneous production of two charmed mesons [28]. They have observed large percentage of the events with two mesons, both containing c quark, with respect to the typical production of the corresponding meson/antimeson pair ($\sigma_{D_i D_j} / \sigma_{D_i \bar{D}_j} \sim 10\%$).

In Ref. [29] we discussed that the large effect is a footprint of double parton scattering. In this paper each step of the double parton scattering was considered in the k_t -factorization approach. In Ref. [30] the authors estimated DPS contribution based on the experimental inclusive D meson spectra measured at the LHC. In their approach fragmentation was included only in terms of the branching fractions for the quark-to-meson transition $c \rightarrow D$. In our approach in Ref. [29] we included full kinematics of hadronization process. There we showed also first differential distributions on the hadron level that can be confronted with recent LHCb experimental data [28].

25 years ago Mueller and Navelet predicted strong decorrelation in relative azimuthal angle [31] of jets with large rapidity separation due to exchange of the BFKL ladder between quarks. The generic picture is presented in diagram (a) of Fig. 2. In a bit simplified picture quark/antiquarks are emitted forward and backward, whereas gluons emitted along the ladder populate rapidity regions in between. Due to diffusion along the ladder the correlation between the most forward and the most backward jets is small. This was a picture obtained within leading-logarithmic BFKL formalism [31, 32, 33, 34, 35, 36]. Calculations of higher-order BFKL effects slightly modified this simple picture [37, 38, 39, 40, 41, 42, 43, 44, 45, 46] leading to smaller decorrelation in rapidity. Recently the NLL corrections were calculated both to the Green's function and to the jet vertices. The effect of the NLL correction is large and leads to significant lowering of the cross section. So far only averaged values of $\langle \cos(n\phi_{jj}) \rangle$ over available phase space or even their ratios were studied experimentally [47]. More detailed studies are necessary to verify this type of calculations. In particular, the approach should reproduce dependence on the rapidity distance between the jets emitted in opposite hemispheres. Large-rapidity-distance jets can be produced only at high energies where the rapidity span is large. A first experimental search for the Mueller-Navelet jets was made by the D0 collaboration. In their study rapidity distance between jets was limited to 5.5 units only. In spite of this they have observed a broadening of the ϕ_{jj} distribution with growing rapidity distance between jets. The dijet azimuthal correlations were also studied in collinear next-to-leading order approximation [48]. The LHC opens new possibility to study the decorrelation effect. First experimental data measured at $\sqrt{s} = 7$ TeV are expected soon [49].

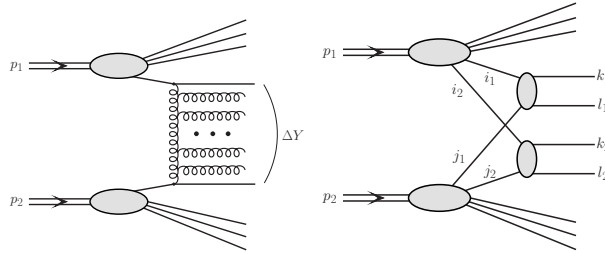


Fig. 2. A diagrammatic representation of the Mueller-Navelet jet production (left diagram) and of the double parton scattering mechanism (right diagram).

The double parton scattering mechanism of W^+W^- production was discussed e.g. in Refs. [11, 50, 51, 52, 53]. The W^+W^- final states constitutes a background to Higgs production. It was discussed recently that double-

parton scattering could explain a large part of the observed signal [54]. We shall also discuss the double parton scattering mechanism of W^+W^- production in the present paper.

2. Formalism used in the calculations

2.1. $c\bar{c}c\bar{c}$ production

Let us consider first production of $c\bar{c}c\bar{c}$ final state within the DPS framework. In a simple probabilistic picture the cross section for double-parton scattering can be written as:

$$\sigma^{DPS}(pp \rightarrow c\bar{c}c\bar{c}X) = \frac{1}{2\sigma_{eff}} \sigma^{SPS}(pp \rightarrow c\bar{c}X_1) \cdot \sigma^{SPS}(pp \rightarrow c\bar{c}X_2). \quad (1)$$

This formula assumes that the two subprocesses are not correlated. At low energies one has to include parton momentum conservation i.e. extra limitations: $x_1 + x_3 < 1$ and $x_2 + x_4 < 1$, where x_1 and x_3 are longitudinal momentum fractions of gluons emitted from one proton and x_2 and x_4 their counterparts for gluons emitted from the second proton. Experimental data [55] provide an estimate of σ_{eff} in the denominator of formula (1). In our studies presented here we usually take $\sigma_{eff} = 15$ mb.

The simple formula (1) can be generalized to address differential distributions. In leading-order approximation differential distribution can be written as

$$\frac{d\sigma}{dy_1 dy_2 d^2p_{1t} dy_3 dy_4 d^2p_{2t}} = \frac{1}{2\sigma_{eff}} \frac{d\sigma}{dy_1 dy_2 d^2p_{1t}} \cdot \frac{d\sigma}{dy_3 dy_4 d^2p_{2t}} \quad (2)$$

which by construction reproduces formula for integrated cross section (1). This cross section is formally differential in 8 dimensions but can be easily reduced to 7 dimensions noting that physics of unpolarized scattering cannot depend on azimuthal angle of the pair or on azimuthal angle of one of the produced c (\bar{c}) quark (antiquark). The differential distributions for each single scattering step can be written in terms of collinear gluon distributions with longitudinal momentum fractions x_1, x_2, x_3 and x_4 expressed in terms of rapidities y_1, y_2, y_3, y_4 and transverse momenta of quark (or antiquark) for each step (in the LO approximation identical for quark and antiquark).

A more general formula for the cross section can be written formally in terms of double-parton distributions, e.g. F_{gg}, F_{qq} , etc. In the case of heavy quark (antiquark) production at high energies:

$$d\sigma^{DPS} = \frac{1}{2\sigma_{eff}} F_{gg}(x_1, x_2, \mu_1^2, \mu_2^2) F_{gg}(x'_1, x'_2, \mu_1^2, \mu_2^2) d\sigma_{gg \rightarrow c\bar{c}}(x_1, x'_1, \mu_1^2) d\sigma_{gg \rightarrow c\bar{c}}(x_2, x'_2, \mu_2^2) dx_1 dx_2 dx'_1 dx'_2. \quad (3)$$

It is rather inspiring to write the double-parton distributions in the impact parameter space $F_{gg}(x_1, x_2, b) = g(x_1)g(x_2)F(b)$, where g are usual conventional parton distributions and $F(b)$ is an overlap of the matter distribution in the transverse plane where b is a distance between both gluons in the transverse plane [56]. The effective cross section in (1) is then $1/\sigma_{eff} = \int d^2b F^2(b)$ and in this approximation is energy independent.

Even if the factorization is valid at some scale, QCD evolution may lead to a factorization breaking. Evolution is known only in the case when the scale of both scatterings is the same [19, 20, 22] i.e. for heavy object, like double gauge boson production.

In Ref. [27] we applied the commonly used in the literature factorized model to $pp \rightarrow c\bar{c}c\bar{c}$ and predicted that at the LHC energies the cross section for two $c\bar{c}$ pair production starts to be of the same size as that for single $c\bar{c}$ production.

In LO collinear approximation the differential distributions for $c\bar{c}$ production depend e.g. on rapidity of quark, rapidity of antiquark and transverse momentum of one of them [27]. In the next-to-leading order (NLO) collinear approach or in the k_t -factorization approach the situation is more complicated as there are more kinematical variables needed to describe the kinematical situation. In the k_t -factorization approach the differential cross section for DPS production of $c\bar{c}c\bar{c}$ system, assuming factorization of the DPS model, can be written as:

$$\frac{d\sigma^{DPS}(pp \rightarrow c\bar{c}c\bar{c}X)}{dy_1 dy_2 d^2p_{1,t} d^2p_{2,t} dy_3 dy_4 d^2p_{3,t} d^2p_{4,t}} = \frac{1}{2\sigma_{eff}} \cdot \frac{d\sigma^{SPS}(pp \rightarrow c\bar{c}X_1)}{dy_1 dy_2 d^2p_{1,t} d^2p_{2,t}} \cdot \frac{d\sigma^{SPS}(pp \rightarrow c\bar{c}X_2)}{dy_3 dy_4 d^2p_{3,t} d^2p_{4,t}}. \quad (4)$$

Again when integrating over kinematical variables one recovers Eq.(1).

$$\sigma_{eff} = \left[\int d^2b (T(\vec{b}))^2 \right]^{-1}, \quad (5)$$

where the overlap function

$$T(\vec{b}) = \int f(\vec{b}_1) f(\vec{b}_1 - \vec{b}) d^2b_1, \quad (6)$$

if the impact-parameter dependent double-parton distributions (dPDFs) are written in the following factorized approximation [22, 57]:

$$\Gamma_{i,j}(x_1, x_2; \vec{b}_1, \vec{b}_2; \mu_1^2, \mu_2^2) = F_{i,j}(x_1, x_2; \mu_1^2, \mu_2^2) f(\vec{b}_1) f(\vec{b}_2). \quad (7)$$

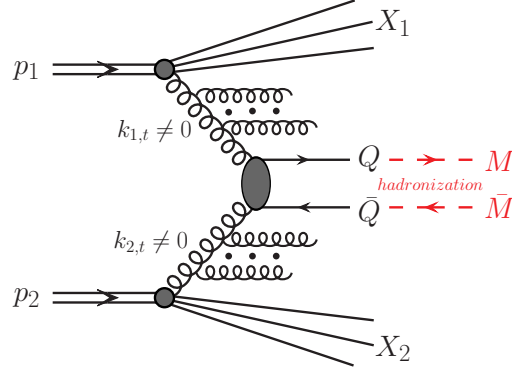


Fig. 3. Production of $c\bar{c}$ quark and antiquark via fusion of virtual gluons.

Without losing generality the impact-parameter distribution can be written as

$$\Gamma(b, x_1, x_2; \mu_1^2, \mu_2^2) = F(x_1, \mu_1^2) F(x_2, \mu_2^2) F(b; x_1, x_2, \mu_1^2, \mu_2^2), \quad (8)$$

where b is the parton separation in the impact parameters space. In the formula above the function $F(b; x_1, x_2, \mu_1^2, \mu_2^2)$ contains all information about correlations between the two partons (two gluons in our case). The dependence was studied numerically in Ref. [57] within Lund Dipole Cascade model. The biggest discrepancy was found in the small b region, particularly for large μ_1^2 and/or μ_2^2 . We shall return to the issue when commenting our results. In general the effective cross section may depend on many kinematical variables:

$$\sigma_{eff}(x_1, x_2, x'_1, x'_2, \mu_1^2, \mu_2^2) = \left(\int d^2b F(b; x_1, x_2, \mu_1^2, \mu_2^2) F(b; x'_1, x'_2, \mu_1^2, \mu_2^2) \right)^{-1}. \quad (9)$$

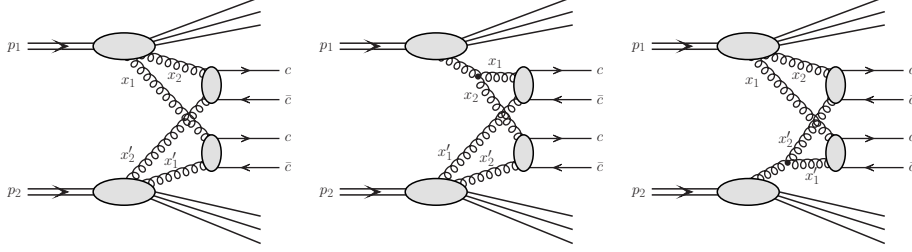
We shall return to these dependences when discussing the role of perturbative parton splitting.

2.2. Parton splitting

In Fig. 4 we illustrate a conventional and perturbative DPS mechanisms for $c\bar{c}c\bar{c}$ production. The 2v1 mechanism (the second and third diagrams) were considered first in [58].

In the case of $c\bar{c}c\bar{c}$ production the cross section for conventional DPS can be written as:

$$\sigma(2v2) = \frac{1}{2} \frac{1}{\sigma_{eff,2v2}} \int dy_1 dy_2 d^2 p_{1t} dy_3 dy_4 d^2 p_{2t} \frac{1}{16\pi\hat{s}^2} |\overline{\mathcal{M}(gg \rightarrow c\bar{c})}|^2 x_1 x'_1 x_2 x'_2$$

Fig. 4. The diagrams for DPS production of $c\bar{c}c\bar{c}$.

$$\times D^{gg}(x_1, x_2, \mu_1^2, \mu_2^2) D^{gg}(x_1, x_2, \mu_1^2, \mu_2^2) \quad (10)$$

while that for the perturbative parton splitting DPS in a very similar fashion (see e.g. [58])

$$\begin{aligned} \sigma(2v1) = & \frac{1}{2} \frac{1}{\sigma_{eff,2v1}} \int dy_1 dy_2 d^2 p_{1t} dy_3 dy_4 d^2 p_{2t} \frac{1}{16\pi\hat{s}^2} \overline{|\mathcal{M}(gg \rightarrow c\bar{c})|^2} x_1 x_1' x_2 x_2' \\ & \times \left(\hat{D}^{gg}(x_1', x_2', \mu_1^2, \mu_2^2) D^{gg}(x_1, x_2, \mu_1^2, \mu_2^2) + D^{gg}(x_1', x_2', \mu_1^2, \mu_2^2) \hat{D}^{gg}(x_1, x_2, \mu_1^2, \mu_2^2) \right) \end{aligned} \quad (11)$$

2.3. Four-jet production in DPS

In the calculations performed in Ref. [59] all partonic cross sections are calculated only in leading order. The cross section for dijet production can be written then as:

$$\frac{d\sigma(ij \rightarrow kl)}{dy_1 dy_2 d^2 p_t} = \frac{1}{16\pi^2 \hat{s}^2} \sum_{i,j} x_1 f_i(x_1, \mu^2) x_2 f_j(x_2, \mu^2) \overline{|\mathcal{M}_{ij \rightarrow kl}|^2}, \quad (12)$$

where y_1, y_2 are rapidities of the two jets and p_t is transverse momentum of one of them (identical).

In our calculations we include all leading-order $ij \rightarrow kl$ partonic subprocesses (see e.g. [60, 61]). The K -factor for dijet production is rather small, of the order of 1.1 – 1.3 (see e.g. [62, 63]), and can be easily incorporated in our calculations. Below we shall show that already the leading-order approach gives results in reasonable agreement with recent ATLAS [64] and CMS [65] data.

This simplified leading-order approach was used in our first estimate of DPS differential cross sections for jets widely separated in rapidity [59]. Similarly as for $c\bar{c}c\bar{c}$ production one can write:

$$\frac{d\sigma^{DPS}(pp \rightarrow 4\text{jets } X)}{dy_1 dy_2 d^2 p_{1t} dy_3 dy_4 d^2 p_{2t}} =$$

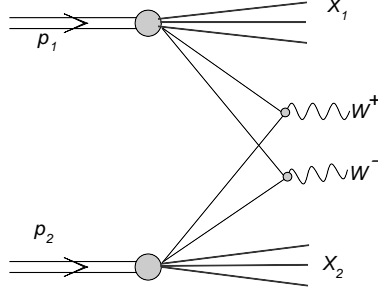


Fig. 5. Diagram representing double parton scattering mechanism of production of W^+W^- pairs.

$$\sum_{i_1, j_1, k_1, l_1, i_2, j_2, k_2, l_2} \frac{\mathcal{C}}{\sigma_{eff}} \frac{d\sigma(i_1 j_1 \rightarrow k_1 l_1)}{dy_1 dy_2 d^2 p_{1t}} \frac{d\sigma(i_2 j_2 \rightarrow k_2 l_2)}{dy_3 dy_4 d^2 p_{2t}}, \quad (13)$$

where $\mathcal{C} = \begin{cases} \frac{1}{2} & \text{if } i_1 j_1 = i_2 j_2 \wedge k_1 l_1 = k_2 l_2 \\ 1 & \text{if } i_1 j_1 \neq i_2 j_2 \vee k_1 l_1 \neq k_2 l_2 \end{cases}$ and partons $j, k, l, m = g, u, d, s, \bar{u}, \bar{d}, \bar{s}$. The combinatorial factors include identity of the two subprocesses. Each step of the DPS is calculated in the leading-order approach (see Eq.(12)). Above y_1, y_2 and y_3, y_4 are rapidities of partons in first and second partonic subprocess, respectively. The p_{1t} and p_{2t} are respective transverse momenta.

Experimental data from the Tevatron [55] and the LHC [66, 28, 67] provide an estimate of σ_{eff} in the denominator of formula (13). As in our recent paper [68] we take $\sigma_{eff} = 15$ mb. A detailed analysis of σ_{eff} based on various experimental data can be found in Refs. [69, 70].

2.4. W^+W^- production

The diagram representating the double parton scattering process is shown in Fig. 5. The cross section for double parton scattering is often modelled in the factorized ansatz which in our case would mean:

$$\sigma_{W^+W^-}^{DPS} = \frac{1}{\sigma_{qq}^{eff}} \sigma_{W^+} \sigma_{W^-}. \quad (14)$$

In general, the parameter σ_{qq} does not need to be the same as for gluon-gluon initiated processes σ_{gg}^{eff} . In the present, rather conservative, calculations we take it to be $\sigma_{qq}^{eff} = \sigma_{gg}^{eff} = 15$ mb. The latter value is known within about 10 % from systematics of gluon-gluon initiated processes at the Tevatron and LHC.

The factorized model (14) can be generalized to more differential distributions. For example in our case of W^+W^- production the cross section differential in W boson rapidities can be written as:

$$\frac{d\sigma_{W^+W^-}^{DPS}}{dy_+ dy_-} = \frac{1}{\sigma_{qq}^{eff}} \frac{d\sigma_W^+}{dy_+} \frac{d\sigma_W^-}{dy_-}. \quad (15)$$

In particular, in leading-order approximation the cross section for quark-antiquark annihilation reads:

$$\begin{aligned} \frac{d\sigma}{dy} = & \sum_{ij} \left(x_1 q_{i/1}(x_1, \mu^2) x_2 \bar{q}_{j/2}(x_2, \mu^2) + x_1 \bar{q}_{i/1}(x_1, \mu^2) x_2 q_{j/2}(x_2, \mu^2) \right) \\ & \times \overline{|\mathcal{M}_{ij \rightarrow W^\pm}|^2} \end{aligned} \quad (16)$$

where the matrix element for quark-antiquark annihilation to W bosons ($\mathcal{M}_{ij \rightarrow W^\pm}$) contains Cabibbo-Kobayashi-Maskawa matrix elements.

When calculating the cross section for single W boson production in leading-order approximation a well known Drell-Yan K -factor can be included. The double-parton scattering would be then multiplied by K^2 .

3. Results for different processes

3.1. $c\bar{c}c\bar{c}$ production

We start presentation of our results with production of two pairs of $c\bar{c}$. In Fig. 6 we compare cross sections for the single and double-parton scattering as a function of proton-proton center-of-mass energy. At low energies the single-parton scattering dominates. For reference we show the proton-proton total cross section as a function of collision energy as parametrized in Ref. [71]. At low energy the $c\bar{c}$ or $c\bar{c}c\bar{c}$ cross sections are much smaller than the total cross section. At higher energies both the contributions dangerously approach the expected total cross section. This shows that inclusion of unitarity effect and/or saturation of parton distributions may be necessary. The effects of saturation in $c\bar{c}$ production were included e.g. in Ref. [72] but not checked versus experimental data. Presence of double-parton scattering changes the situation. The double-parton scattering is potentially very important ingredient in the context of high energy neutrino production in the atmosphere [73, 74, 72] or of cosmogenic origin [75]. At LHC energies the cross section for both terms become comparable. This is a completely new situation.

So far we have concentrated on DPS production of $c\bar{c}c\bar{c}$ and completely ignored SPS production of $c\bar{c}c\bar{c}$. In Refs.[76, 68] we calculated the SPS contribution in high-energy approximation [76] and including all diagrams

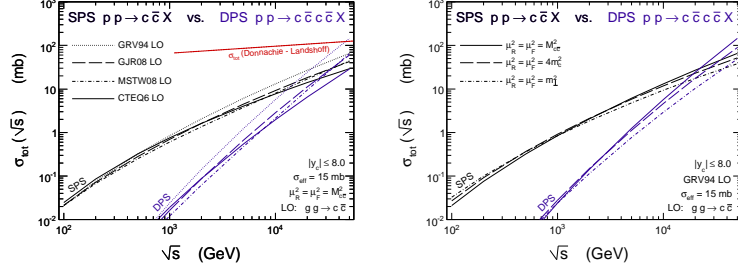


Fig. 6. Total LO cross section for $c\bar{c}$ and double-parton scattering production of $c\bar{c}c\bar{c}$ as a function of center-of-mass energy (left panel) and uncertainties due to the choice of (factorization, renormalization) scales (right panel). We show in addition a parametrization of the total cross section in the left panel.

in the collinear-factorization approach [68]. In Fig. 7 we show the cross section from Ref. [68]. The corresponding cross section at the LHC energies is more than two orders of magnitude smaller than that for $c\bar{c}$ production i.e. much smaller than the DPS contribution discussed in the previous figure.

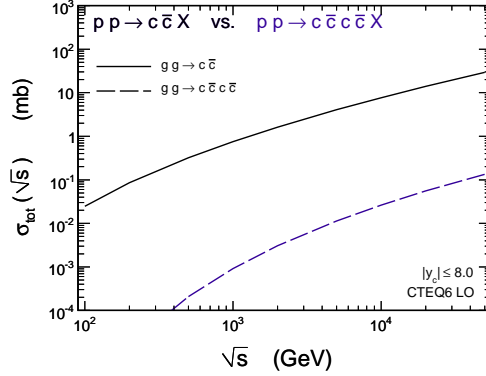


Fig. 7. Cross section for SPS production of $c\bar{c}c\bar{c}$ compared to this for standard $c\bar{c}$ production as a function of collision energy.

In experiment one measures D mesons instead of charm quarks/antiquarks. In Fig. 8 we show resulting distributions in rapidity distance between two D^0 mesons (left panel) and corresponding distribution in relative azimuthal angle (right panel). The DPS contribution (dashed line) dominates over the single parton scattering one (dash-dotted line). The sum of the two contributions is represented by the solid line. We get a reasonable agreement

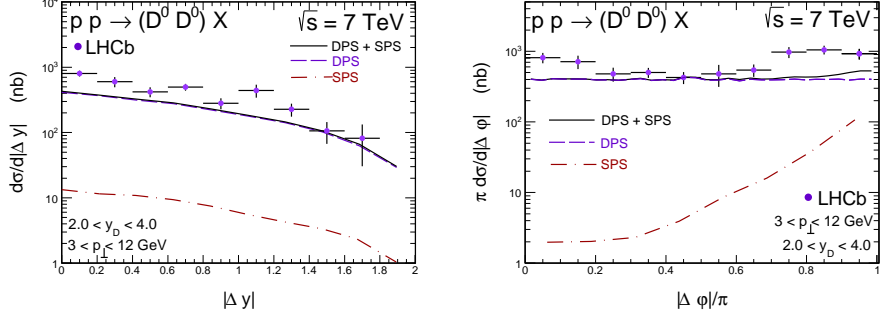


Fig. 8. Rapidity distance between two D^0 mesons (left panel) and corresponding azimuthal correlations (right panel).

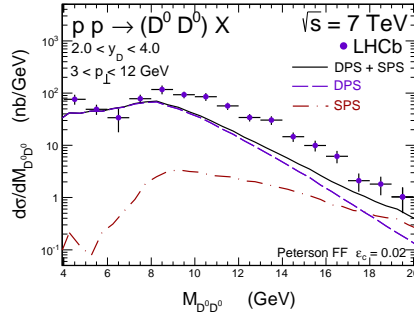


Fig. 9. Distribution of invariant mass of two D^0 mesons.

with the LHCb experimental data [28].

Distribution in the invariant mass of two $D^0 D^0$ mesons is shown in Fig. 9. Again a reasonable agreement is obtained. Some strength is missing in the interval $10 \text{ GeV} < M_{D^0 D^0} < 16 \text{ GeV}$.

At the LHC the cross section for $pp \rightarrow c\bar{c}$ is still bigger than that for $pp \rightarrow c\bar{c}c\bar{c}$ [29]. As shown in Fig. 6 the latter cross section is growing fast and at high energy it may become even larger than that for single pair production. The situation at Future Circular Collider (FCC) is shown in Fig. 10. Now the situation reverses and the cross section for $c\bar{c}c\bar{c}$ is bigger than that for single pair production. We predict rather flat distributions in charm quark/antiquark rapidities. The shapes in quark/antiquark transverse momenta are almost identical which can be easily understood within the formalism presented in the previous section.

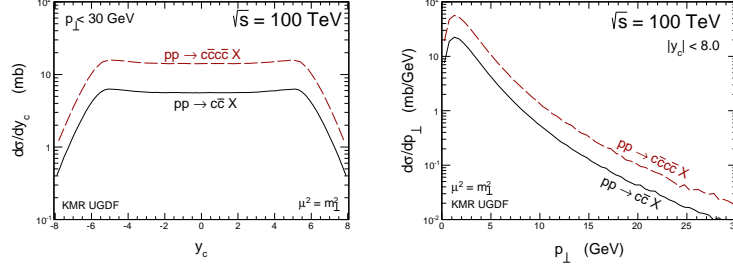


Fig. 10. Cross section for one c or one \bar{c} from the $c\bar{c}c\bar{c}$ final state at the FCC.

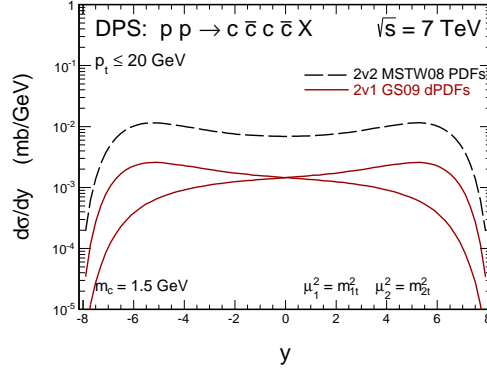


Fig. 11. Rapidity distribution of charm quark/antiquark for $\sqrt{s} = 7$ TeV for $\mu_1^2 = m_{1t}^2$, $\mu_2^2 = m_{2t}^2$.

3.2. Parton splitting

As described in the Formalism section the splitting contributions are calculated in leading order only. In the calculations performed in Ref. [58] we either assumed $\mu_1^2 = m_{1t}^2$ and $\mu_2^2 = m_{2t}^2$, or $\mu_1^2 = M_{c\bar{c},1}^2$ and $\mu_2^2 = M_{c\bar{c},2}^2$. The quantity m_{it} is the transverse mass of either parton emerging from subprocess i , whilst $M_{c\bar{c},i}$ is the invariant mass of the pair emerging from subprocess i .

In Fig. 11 we show the rapidity distribution of the charm quark/antiquark for different choices of the scale at $\sqrt{s} = 7$ TeV. The conventional and splitting terms are shown separately. The splitting contribution (lowest curve, red online) is smaller, but has almost the same shape as the conventional DPS contribution. We can observe asymmetric (in rapidity) shapes for the $1v2$ and $2v1$ contributions.

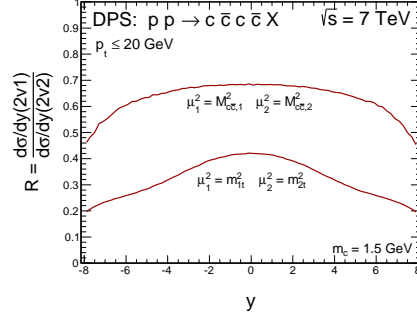


Fig. 12. Ratio of the 2v1 to 2v2 cross sections as a function of quark/antiquark rapidity.

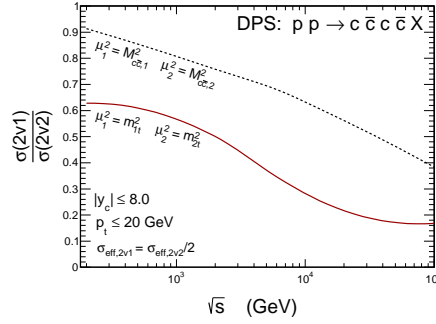


Fig. 13. Ratio of the 2v1 to 2v2 cross sections as a function of collision energy.

The corresponding ratios of the 2v1-to-2v2 contributions as a function of rapidity is shown in Fig. 12.

In Fig. 13 we show energy dependence of the ratio of the 2v1 to 2v2 cross sections. The ratio systematically decreases with the collision energy.

Finally in Fig. 14 we show the empirical σ_{eff} , for double charm production. Again σ_{eff} rises with the centre-of-mass energy. A sizeable difference of results for different choices of scales can be observed.

3.3. Jets with large rapidity separation

In Fig. 15 we compare our calculation for inclusive jet production with the CMS data [65]. In addition, we show contributions of different partonic mechanisms. In all rapidity intervals the gluon-gluon and quark-gluon (gluon-quark) contributions clearly dominate over the other contributions

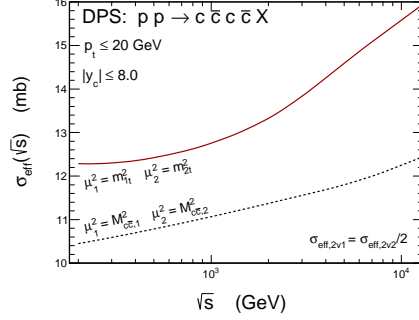


Fig. 14. Energy and factorization scale dependence of σ_{eff} for $c\bar{c}c\bar{c}$ production as a consequence of existence of the two DPS components. In this calculation $\sigma_{eff,2v2} = 30$ mb and $\sigma_{eff,2v1} = 15$ mb.

and in practice it is sufficient to include only these subprocesses in further analysis.

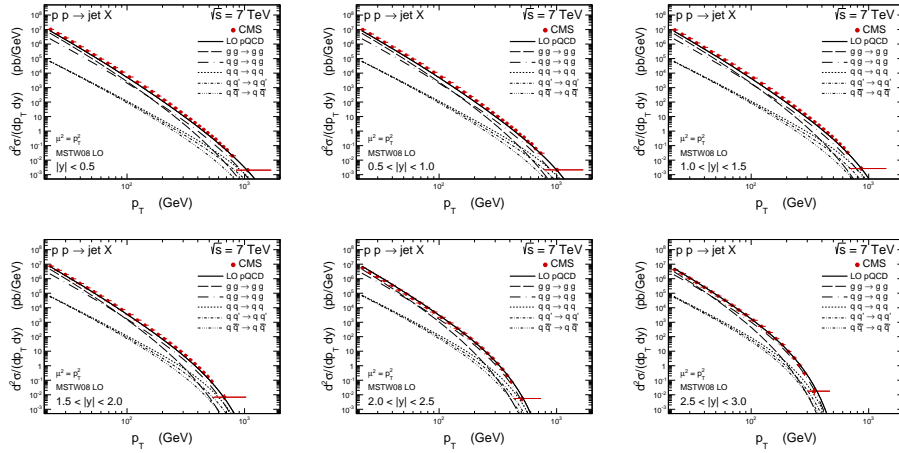


Fig. 15. Our results for inclusive jet production against the CMS experimental data [65]. In addition we show decomposition into different partonic components as explained in the figure caption.

Now we proceed to the jets with large rapidity separation. In Fig. 16 we show distribution in the rapidity distance between two jets in leading-order collinear calculation and between the most distant jets in rapidity in the case of four DPS jets. In this calculation we have included cuts for the

CMS experiment [49]: $y_1, y_2 \in (-4.7, 4.7)$, $p_{1t}, p_{2t} \in (35 \text{ GeV}, 60 \text{ GeV})$. For comparison we show also results for the BFKL calculation from Ref. [44]. For this kinematics the DPS jets give sizeable contribution only at large rapidity distance. The NLL BFKL cross section (long-dashed line) is smaller than that for the LO collinear approach (short-dashed line).

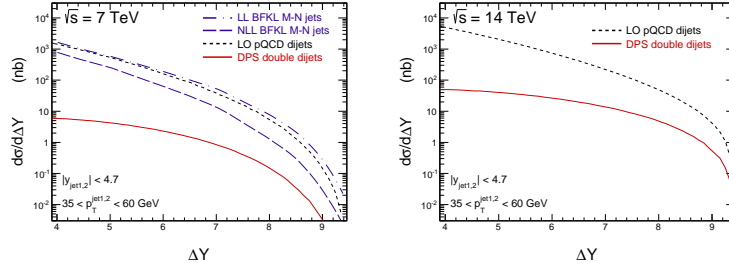


Fig. 16. Distribution in rapidity distance between jets ($35 \text{ GeV} < p_t < 60 \text{ GeV}$) with maximal (the most positive) and minimal (the most negative) rapidities. The collinear pQCD result is shown by the short-dashed line and the DPS result by the solid line for $\sqrt{s} = 7 \text{ TeV}$ (left panel) and $\sqrt{s} = 14 \text{ TeV}$ (right panel). For comparison we show also results for the BFKL Mueller-Navelet jets in leading-logarithm and next-to-leading-order logarithm approaches from Ref. [44].

In Fig. 17 we show rapidity-distance distribution for even smaller lowest transverse momenta of the "jet". A measurement of such minijets may be, however, difficult. Now the DPS contribution may even exceed the standard SPS dijet contribution, especially at the nominal LHC energy. How to measure such (mini)jets is an open issue. In principle, one could measure correlations of semihard ($p_t \sim 10 \text{ GeV}$) neutral pions with the help of so-called zero-degree calorimeters (ZDC) which are installed by all major LHC experiments.

3.4. Production of W^+W^- pairs

It was argued that the DPS contribution for inclusive W^+W^- could be large [54]. Here we partly report results from Ref. [52]. In this analysis we have assumed $\sigma_{eff} = 15 \text{ mb}$ as is a phenomenological standard for many other, mostly gluon-gluon induced, processes. Similar value was used also in other recent analysis [53] where in addition evolution effects of dPDFs were discussed. In our opinion the normalization of the cross section may be an open issue [52]. Therefore below we wish to compare rather shapes of a few distributions. In Fig. 18 we show two-dimensional distributions in rapidity of W^+ and W^- . For reference we show also distributions for $\gamma\gamma$ and $q\bar{q}$

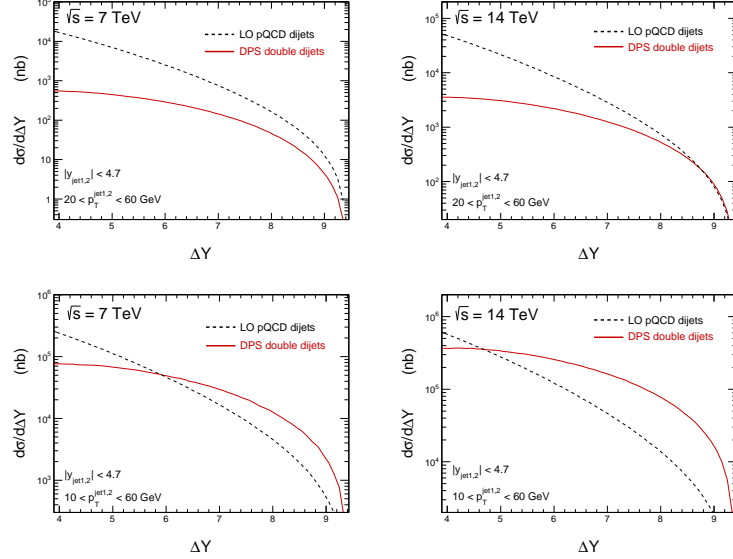


Fig. 17. The same as in the previous figure but now for somewhat smaller lower cut on minijet transverse momentum.

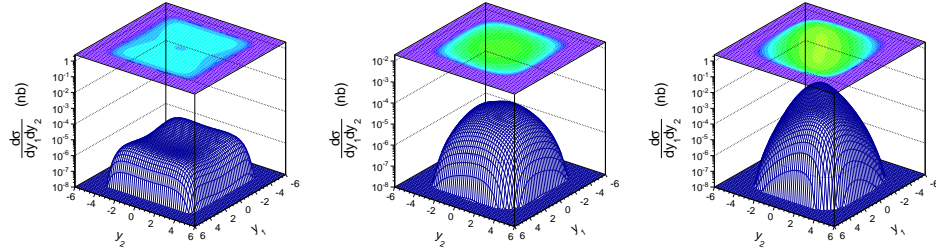


Fig. 18. Two-dimensional distributions in rapidity of W^+ and rapidity of W^- for the DPS mechanism (left), $\gamma\gamma$ (middle) and $q\bar{q}$ (right) mechanism for $\sqrt{s} = 8$ TeV.

components (see a detailed discussion in Ref. [52]). The DPS contribution seems broader in the (y_{W^+}, y_{W^-}) space than the other two contributions.

In Fig. 19 we show invariant M_{WW} mass distribution for $\sqrt{s} = 8$ TeV. The DPS contribution seems to dominate at very large invariant masses.

How the situation may look at future high-energy experiments at the LHC and FCC is shown in Table 1 and Fig. 20. Now the DPS (conservative estimation) is relatively larger compared to other contributions.

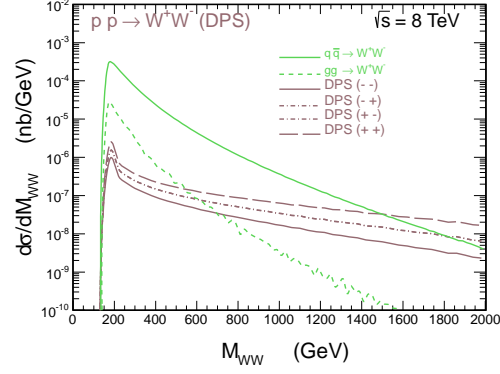


Fig.19. M_{WW} invariant mass distribution for different mechanism discussed in Ref. [52].

Table 1. Cross section for W^+W^- production at different collision energies for the dominant $q\bar{q}$ and DPS contributions.

	$q\bar{q}$	DPS
8000	0.032575	0.1775(-03)
14000	0.06402	0.6367(-03)
100000	0.53820	0.03832

In experiments one can measure charged leptons and not W^\pm bosons.

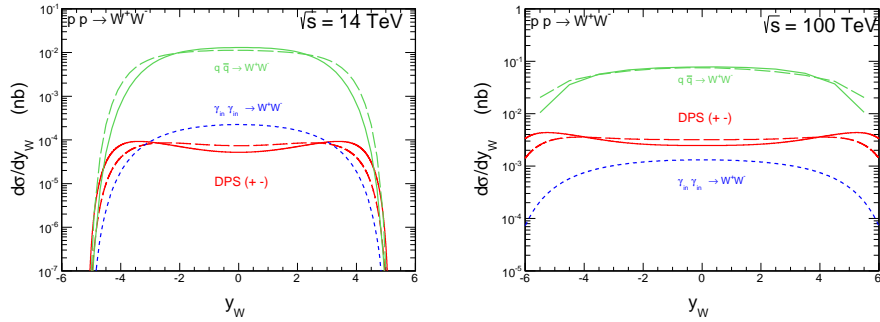


Fig. 20. Our predictions for future experiments.

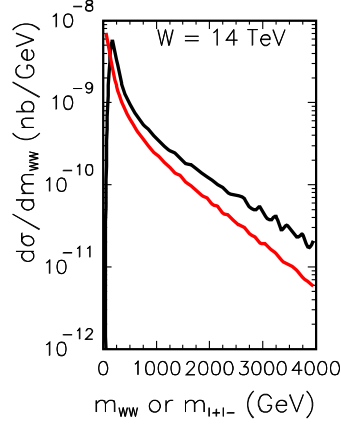


Fig. 21. Invariant mass distribution of the W^+W^- system (thick solid line) and corresponding distribution for the $\mu^+\mu^-$ system. No branching fractions are included.

Therefore a detailed study of lepton distributions is needed. As an example we show (see Fig. 21) distribution of invariant mass of charged leptons compared with that for gauge bosons. Only a relatively small shift towards smaller invariant masses is observed. A more detailed studies are necessary to answer whether the W^+W^- distribution can be identified experimentally. Several background contributions have to be considered. We leave such a detailed studies for future.

4. Conclusions

We have briefly review some double-parton scattering processes considered by us recently.

First we have shown, within a leading-order collinear-factorization, that the cross section for $c\bar{c}c\bar{c}$ production grows much faster than the cross section for $c\bar{c}$ making the production of two pairs of $c\bar{c}$ production very attractive in the context of exploring the double-parton scattering processes.

We have also discussed production of $c\bar{c}c\bar{c}$ in the double-parton scattering in the factorized Ansatz with each step calculated in the k_t -factorization approach, i.e. including effectively higher-order QCD corrections.

The cross section for the same process calculated in the k_t -factorization approach turned out to be larger than its counterpart calculated in the LO collinear approach.

We have calculated also cross sections for the production of $D_i D_j$ (both containing c quark) and $\bar{D}_i \bar{D}_j$ (both containing \bar{c} antiquark) pairs of mesons. The results of the calculation have been compared to recent results of the LHCb collaboration.

The total rates of the meson pair production depend on the unintegrated gluon distributions. The best agreement with the LHCb data has been obtained for the Kimber-Martin-Ryskin UGDF. This approach, as discussed already in the literature, effectively includes higher-order QCD corrections.

As an example we have shown some differential distributions for $D^0 \bar{D}^0$ pair production. Rather good agreement has been obtained for transverse momentum distribution of D^0 (\bar{D}^0) mesons and $D^0 \bar{D}^0$ invariant mass distribution. The distribution in azimuthal angle between both D^0 's suggests that some contributions may be still missing. The single parton scattering contribution, calculated in the high energy approximation, turned out to be rather small. In the meantime we checked that $2 \rightarrow 4$ ($gg \rightarrow c\bar{c}c\bar{c}$) k_t -factorization approach leads to similar results as the collinear approach discussed here [77].

We have discussed also a new type of mechanism called parton splitting in the context of the $c\bar{c}c\bar{c}$ production. Our calculation showed that the parton-splitting contribution gives sizeable contribution and has to be included when analysing experimental data. However, it is too early in the moment for precise predictions of the corresponding contributions as our results strongly depend on the values of not well known parameters $\sigma_{eff,2v2}$ and $\sigma_{eff,2v1}$. Some examples inspired by a simple geometrical model of colliding partons have been shown. A better understanding of the two non-perturbative parameters is a future task.

We have shown that almost all differential distributions for the conventional and the parton-splitting contributions have essentially the same shape. This makes their model-independent separation extremely difficult. This also shows why the analyses performed so far could describe different experimental data sets in terms of the conventional 2v2 contribution alone. The sum of the 2v1 and 2v2 contributions behaves almost exactly like the 2v2 contribution, albeit with a smaller σ_{eff} that depends only weakly on energy, scale and momentum fractions. With the perturbative 2v1 mechanism included, σ_{eff} increases as \sqrt{s} is increased, and decreases as Q is increased.

We have discussed also how the double-parton scattering effects may contribute to large-rapidity-distance dijet correlations. The presented results were performed in leading-order approximation only i.e. each step of DPS was calculated in collinear pQCD leading-order. Already leading-order calculation provides quite adequate description of inclusive jet production when confronted with recent results obtained by the ATLAS and CMS col-

laborations. We have identified the dominant partonic pQCD subprocesses relevant for the production of jets with large rapidity distance.

We have shown distributions in rapidity distance between the most-distant jets in rapidity. The results of the dijet SPS mechanism have been compared to the DPS mechanism. We have performed calculations relevant for a planned CMS analysis. The contribution of the DPS mechanism increases with increasing distance in rapidity between jets.

We have also shown some recent predictions of the Mueller-Navelet jets in the LL and NLL BFKL framework from the literature. For the CMS configuration our DPS contribution is smaller than the dijet SPS contribution even at high rapidity distances and only slightly smaller than that for the NLL BFKL calculation known from the literature. The DPS final state topology is clearly different than that for the dijet SPS (four versus two jets) which may help to disentangle the two mechanisms experimentally.

We have shown that the relative effect of DPS can be increased by lowering the transverse momenta. Alternatively one could study correlations of semihard pions distant in rapidity. Correlations of two neutral pions could be done, at least in principle, with the help of so-called zero-degree calorimeters present at each main detectors at the LHC.

The DPS effects are interesting not only in the context how they contribute to distribution in rapidity distance but per se. One could make use of correlations in jet transverse momenta, jet imbalance and azimuthal correlations to enhance the contribution of DPS. Further detailed Monte Carlo studies are required to settle real experimental program of such studies. The four-jet final states analyses of distributions in rapidity distance and other kinematical observables was performed by us very recently [78].

Finally we have discussed DPS effects in inclusive production of W^+W^- pairs. We have shown that the relative contribution of DPS grows with collision energy. In experiments one measures rather electrons or muons than the gauge bosons. Whether experimental identification of the DPS contribution in this case is possible requires a detailed Monte Carlo studies.

Acknowledgments

This presentation is based on common work mostly with Rafał Maciuła and partially with Jonathan Gaunt, Marta Luszczak and Wolfgang Schäfer. I am very indebted to Rafał Maciuła for help in preparing this manuscript.

REFERENCES

- [1] P.V. Landshoff and J.C. Polinghorne, Phys. Rev. **D18** (1978) 3344.

- [2] F. Takagi, Phys. Rev. Lett. **18** (1979) 1296.
- [3] C. Goebel and D.M. Scott and F. Halzen, Phys. Rev. **D22** (1980) 2789.
- [4] B. Humpert, Phys. Lett. **B131** (1983) 461.
- [5] N. Paver and D. Treleani, Phys. Lett. **B146** (1984) 252.
- [6] N. Paver and D. Treleani, Z. Phys. **C28** (1985) 187.
- [7] M. Mekhfi, Phys. Rev. **D32** 2371; M. Mekhfi, Phys. Rev. **D32** 2380.
- [8] B. Humpert and R. Oderico, Phys. Lett. **B154** (1985) 211.
- [9] T. Sjöstrand and M. van Zijl, Phys. Rev. **D36** (1987) 2019.
- [10] M. Drees and T. Han, Phys. Rev. Lett. **77** (1996) 4142.
- [11] A. Kulesza and W.J. Stirling, Phys. Lett. **B475** (2000) 168.
- [12] A. Del Fabbro and D. Treleani, Phys. Rev. **D66** (2002) 074012.
- [13] E.L. Berger, C.B. Jackson and G. Shaughnessy, Phys. Rev. **D81** 014014 (2010).
- [14] J.R. Gaunt, C-H. Kom, A. Kulesza and W.J. Stirling, arXiv:1003.3953.
- [15] M. Strikman and W. Vogelsang, Phys. Rev. **D83** (2011) 034029.
- [16] B. Blok, Yu. Dokshitzer, L. Frankfurt and M. Strikman, Phys. Rev. **D83** (2011) 071501.
- [17] C.H. Khom, A. Kulesza and W.J. Stirling, Phys. Rev. Lett. **107** (2011) 082002.
- [18] S.R. Baranov, A. M. Snigirev and N.P. Zotov, arXiv:1105.6279.
- [19] A.M. Snigirev, Phys. Rev. **D68** (2003) 114012.
- [20] V.L. Korotkikh and A.M. Snigirev, Phys. Lett. **B594** (2004) 171.
- [21] T. Sjöstrand and P.Z. Skands, JHEP **0403** (2004) 053.
- [22] J.R. Gaunt and W.J. Stirling, JHEP **1003** (2010) 005.
- [23] J.R. Gaunt and W.J. Stirling, JHEP **1106** (2011) 048.
- [24] M. Diehl and A. Schäfer, Phys. Lett. **B698** (2011) 389.
- [25] M.G. Ryskin and A.M. Snigirev, Phys. Rev. **D83** (2011) 114047.
- [26] M. Diehl, D. Ostermeier and A. Schäfer, arXiv:1111.0910.
- [27] M. Łuszczak, R. Maciula and A. Szczurek, Phys. Rev. **D85** (2012) 094034.
- [28] R. Aaij *et al.* [LHCb Collaboration], J. High Energy Phys. **06**, 141 (2012); J. High Energy Phys **03**, 108 (2014); [arXiv:1205.0975 [hep-ex]].
- [29] R. Maciula and A. Szczurek, Phys. Rev. **D87** (2013) 074039.
- [30] A.V. Berezhnoy et al., Phys. Rev. **D86** (2012) 034017.
- [31] A. H. Mueller, and H. Navelet, Nucl. Phys. **B282**, 727 (1987).
- [32] V. Del Duca and C. R. Schmidt, Phys. Rev. **D49**, 4510 (1994); arXiv:9311290 [hep-ph].
- [33] W. J. Stirling, Nucl. Phys. **B423**, 56 (1994); arXiv:9401266 [hep-ph].
- [34] V. Del Duca and C. R. Schmidt, Phys. Rev. **D51**, 2150 (1995); arXiv:9407359 [hep-ph].

- [35] V. T. Kim and G. B. Pivovarov, Phys. Rev. **D 53**, 6 (1996); arXiv:9506381 [hep-ph].
- [36] J. Andersen, V. Del Duca, S. Frixione, C. Schmidt and W. J Stirling, J. High Energy Phys. **02**, 007 (2001); arXiv:0101180 [hep-ph].
- [37] J. Bartels, D. Colferai and G. Vacca, Eur. Phys. J. **C24**, 83 (2002); Eur. Phys. J. **C 29**, 235 (2003).
- [38] A. Sabio Vera and F. Schwennsen, Nucl. Phys. **B776**, 170 (2007); arXiv:0702158 [hep-ph].
- [39] C. Marquet and C. Royon, Phys. Rev. **D79**, 034028 (2009); arXiv:0704.3409 [hep-ph].
- [40] D. Colferai, F. Schwennsen, L. Szymanowski and S. Wallon, J. High Energy Phys. **12**, 026 (2010); arXiv:1002.1365 [hep-ph].
- [41] F. Caporale, D. Y. Ivanov, B. Murdaca, A. Papa and A. Perri, J. High Energy Phys. **02**, 101 (2012); arXiv:1112.3752 [hep-ph].
- [42] D. Y. Ivanov and A. Papa, J. High Energy Phys. **05**, 086 (2012); arXiv:1202.1082 [hep-ph].
- [43] F. Caporale, D. Y. Ivanov, B. Murdaca and A. Papa, Nucl. Phys. **B877**, 73 (2013); arXiv:1211.7225 [hep-ph].
- [44] B. Ducloue, L. Szymanowski and S. Wallon, J. High Energy Phys. **05**, 096 (2013); arXiv:1302.7012 [hep-ph].
- [45] B. Duclou, L. Szymanowski and S. Wallon, Phys. Rev. Lett. **112**, 082003 (2014); arXiv:1309.3229 [hep-ph].
- [46] V. Del Duca, L. J. Dixon, C. Duhr, J. Pennington, J. High Energy Phys. **02**, 086 (2014); arXiv:1309.6647.
- [47] S. Chatrchyan et al. (the CMS Collaboration), CMS-PAS-FSQ-12-002 (2013).
- [48] P. Aurenche, R. Basu and M. Fontannaz, Eur. Phys. J. **C57**, 681 (2008); arXiv:0807.2133 [hep-ph].
- [49] I. Pozdnyakov, private communication
- [50] J.R. Gaunt, Ch.-H. Kom, A. Kulesza and W.J. Stirling, Eur. Phys. J. **C69** (2010) 53, arXiv:1003.3953 [hep-ph].
- [51] J.R. Gaunt, Ch.-H. Kom, A. Kulesza and W.J. Stirling, arXiv:1110.1174 [hep-ph].
- [52] M. Luszczak, A. Szczurek and C. Royon, J. High Energy Phys. **02**, 098 (2015); [arXiv:1409.1803 [hep-ph]].
- [53] K. Golec-Biernat and E. Lewandowska, Phys. Rev. **D90** (2014) 094032.
- [54] W. Krasny and W. Płaczek, Acta Phys. Pol. **B45** (2014) 71, arXiv:1305.1769 [hep-ph].
- [55] F. Abe et al. (CDF Collaboration), Phys. Rev. **D56**, 3811 (1997); Phys. Rev. Lett. **79**, 584 (1997); V. M. Abazov, Phys. Rev. **D81**, 052012 (2010).
- [56] G. Calucci and D. Treleani, Phys. Rev. **D60** (1999) 054023.

- [57] C. Flensburg, G. Gustafson, L. Lonnblad and A. Ster, J. High Energy Phys. **06**, 066 (2011); [arXiv:1103.4320 [hep-ph]].
- [58] J.R. Gaunt, R. Maciula and A. Szczurek, Phys. Rev. **D90** (2014) 054017.
- [59] R. Maciula and A. Szczurek, Phys. Rev. D **90**, 014022 (2014) [arXiv:1403.2595 [hep-ph]].
- [60] R. K. Ellis, W. J. Stirling and B. R. Webber, Camb. Monogr. Part. Phys. Nucl. Phys. Cosmol. **8** (1996) 1-435.
- [61] V. D. Barger and R. J. N. Phillips, Redwood City, USA: Addison-Wesley (1987) 592 p. (Frontiers in Physics, 71).
- [62] J. M. Campbell, J. W. Huston and W. J. Stirling, Rept. Prog. Phys. **70**, 89 (2007); arXiv:0611148 [hep-ph].
- [63] A. Gehrmann-De Ridder, T. Gehrmann, E. W. N. Glover and J. Pires, Phys. Rev. Lett. **110**, 162003 (2013); arXiv:1301.7310 [hep-ph].
- [64] G. Aad et al. (the ATLAS collaboration), Eur. Phys. J. **C 71**, 1512 (2011).; arXiv:1009.5908 [hep-ex]
- [65] S. Chatrchyan et al. (the CMS collaboration), Phys. Rev. Lett. **107**, 132001 (2011); arXiv:1106.0208 [hep-ex].
- [66] R. Aaij *et al.* [LHCb Collaboration], Phys. Lett. B **707**, 52 (2012) [arXiv:1109.0963 [hep-ex]].
- [67] G. Aad *et al.* [ATLAS Collaboration], New J. Phys. **15**, 033038 (2013) [arXiv:1301.6872 [hep-ex]].
- [68] A. van Hameren, R. Maciula and A. Szczurek, Phys. Rev. D **89**, 094019 (2014); arXiv:1402.6972 [hep-ph].
- [69] M. H. Seymour and A. Siodmok, J. High Energy Phys. **10**, 113 (2013); arXiv:1307.5015 [hep-ph].
- [70] M. Bahr, M. Myska, M. H. Seymour and A. Siodmok, J. High Energy Phys. **03**, 129 (2013); arXiv:1302.4325 [hep-ph].
- [71] A. Donnachie and P.V. Landshoff, Phys. Lett. **B296** (1992) 227.
- [72] R. Enberg, M.H. Reno and I. Sarcevic, Phys. Rev. **D78** (2008) 043005.
- [73] P. Gondolo, G. Ingelman and M. Thunman, Astropart. Phys. **5** (1996) 309; Nucl. Phys. Proc. Suppl. **43** (1995) 274; Nucl. Phys. Proc. Suppl. **48** (1996) 472.
- [74] A.D. Martin, M.G. Ryskin and A.M. Stasto, Acta Phys. Polon. B **34** (2003) 3273.
- [75] R. Enberg, M.H. Reno and I. Sarcevic, Phys. Rev. **D79** (2009) 053006.
- [76] W. Schäfer and A. Szczurek, Phys. Rev. **D85** (2012) 094029.
- [77] A. van Hameren, R. Maciula and A. Szczurek, a paper in preparation.
- [78] R. Maciula and A. Szczurek, arXiv:1503.08022 [hep-ph].